DOI: 10.1002/cbic.200800617

Metal Binding Properties of Fluorescent Analogues of Trichogin GA IV: A Conformational Study by Time-Resolved Spectroscopy and Molecular Mechanics Investigations

Mariano Venanzi,*[a] Gianfranco Bocchinfuso,[a] Emanuela Gatto,[a] Antonio Palleschi,[a] Lorenzo Stella,[a] Fernando Formaggio,[b] and Claudio Toniolo[b]

The metal ion binding properties of two fluorescent analogues of trichogin GA IV, which is a natural undecapeptide showing significant antimicrobial activity, were studied by circular dichroism, time-resolved optical spectroscopy, and molecular mechanics calculations. Binding of Ca^{II} and Gd^{III} to the peptides investigated was shown to promote a structural transition from highly helical conformations to folded structures characterized by formation of a loop that embedded the metal ion. Time-resolved spectroscopy revealed that peptide dynamics is also remarkably affected by ion binding: peptide-backbone motions slowed down to the microsecond time scale. Finally, molecular mechanics calculations emphasized the role of the central Gly5-Gly6 motif, which allowed for the twisting of the peptide segment that gave rise to the formation of the binding cavity.

Introduction

Trichogin GA IV (TrGA) is the prototype molecule of lipopeptaibols, a unique group of naturally occurring oligopeptides exhibiting a remarkable antimicrobial activity.[1–3] The primary structure of TrGA, that is, Oct-Aib-Gly-Leu-Aib-Gly-Gly-Leu-Aib-Gly-Ile-Lol (Oct = 1-octanoyl; Aib = α-aminoisobutyric acid; Lol = leucinol), which comprises three Aib and four Gly residues, anticipates the peculiar structural and dynamic properties of this peptide. The Aib residues, due to the gem-dimethyl substitution on their C^{α} atom,[4–7] are well known to favour the formation of 3_{10}/α-helical structures[8] and β turns,[9] while the Gly residues confer conformational flexibility to the peptide backbone. X-ray diffraction data showed that the first four residues at the N terminus attain a right-handed 3_{10}-helix, while the C-terminal segment, next to the Gly5-Gly6 motif, populates a right-handed α-helix.[10] NMR spectroscopy and CD studies suggested that this 3_{10}/α-helix mixed conformation is basically maintained in solution, although the C-terminal region was found to be in equilibrium with unordered states.[11–13] Recently, we investigated the conformational and dynamic properties in solution of fluorescent labelled TrGA analogues by time-resolved optical spectroscopies and molecular mechanics (MM) calculations, and showed that a conformational transition from an elongated, helical conformation to a family of compact, folded structures that mimic a helix-turn-helix motif, takes place in the microsecond time regime.[14,15]

The close similarity of these folded conformers to the helix-loop-helix motif of a number of calcium-binding proteins and peptides[16,17] urged us to investigate the metal-ion binding properties of these TrGA analogues. Besides Ca^{II}, we selected Gd^{III} for its well-known properties as a magnetic probe and because due to its similar radius and coordination properties is the best substitute for calcium.[18] Furthermore, the efficiency of Gd^{III} in NMR contrast imaging has been shown to greatly increase when embedded in a membrane phase.[19] Our ultimate goal is therefore to exploit the extremely high affinity of TrGA for the lipid phase in the transport of paramagnetic Gd^{III} ions into the membrane for achieving better contrast conditions in magnetic imaging.

Here, we report on the structural and dynamic properties of the ion–peptide complexes formed by two different fluorescent analogues of TrGA with Ca^{II} and Gd^{III}. The peptides investigated, denoted as F0 and F0T8 (Scheme 1), were both functionalized with a fluorescent molecule (Fmoc: fluoren-9-ylmethyloxycarbonyl), which replaced the Oct group at the N terminus of TrGA. In F0T8 a TOAC (4-amino-1-oxyl-2,2,6,6-tetramethylpiperidine-4-carboxylic acid) residue, a C^{α}-tetrasubstituted α-amino acid bearing a nitroxide radical species in the side chain, was used to replace Aib at position 8. It has already been reported that while substitution of the Fmoc group does not affect the conformational properties of the trichogin analogues, inclusion of TOAC in the C-terminal segment slightly stabilizes the helical conformation.[15] Permeabilization experiments on phospholipid bilayers proved that the above substitutions do not perturb the membrane activity of the peptides investigated.[14]

[a] *Prof. M. Venanzi, Dr. G. Bocchinfuso, Dr. E. Gatto, Prof. A. Palleschi, Prof. L. Stella*
Department of Chemical Sciences and Technologies
University of Rome "Tor Vergata"
Via della Ricerca Scientifica, 00133 Rome (Italy)
Fax: (+39) 06-7259-4328
E-mail: venanzi@uniroma2.it

[b] *Prof. F. Formaggio, Prof. C. Toniolo*
Institute of Biomolecular Chemistry, CNR, Padova Unit
Department of Chemistry, University of Padova
Via Marzolo 1, 35131 Padova (Italy)
Fax: (+39) 049-827-5239

Supporting information for this article is available on the WWW under http://dx.doi.org/10.1002/cbic.200800617 or from the author.

Fmoc-Aib-Gly-Leu-Aib-Gly-Gly-Leu-Aib-Gly-Ile-Leu-OMe (F0)

Fmoc-Aib-Gly-Leu-Aib-Gly-Gly-Leu-**TOAC**-Gly-Ile-Leu-OMe (F0T8)

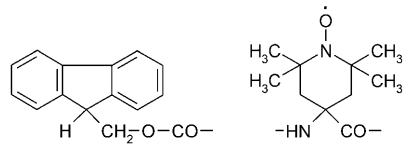

Scheme 1. The primary structures of the two trichogin GA IV analogues, F0 and F0T8, investigated. The molecular structures of fluoren-9-ylmethyloxycarbonyl (Fmoc) and 4-amino-1-oxyl-2,2,6,6-tetramethylpiperidine-4-carboxylic acid (TOAC) are also shown; Aib: α-aminoisobutyric acid.

The well-established distance dependence of the Fmoc···TOAC excited-state interaction allowed us to investigate the conformational and dynamic properties of F0T8 in methanol by combining fluorescence resonance energy transfer (FRET) experiments and MM calculations.[14,15] Information on the peptide dynamics in the microsecond time region was also obtained from time-resolved transient absorption measurements by analysing the quenching of the Fmoc triplet state decay by TOAC. Summarising the principal findings of our previous investigations, we showed that the F0T8 dynamics in the microsecond time region is determined by a conformational transition from an extended helical conformation, similar to the $3_{10}/\alpha$-helix mixed conformation revealed by X-ray diffraction and NMR spectroscopy studies, to a family of compact, folded structures characterized by a β bend involving the Aib4-Gly5-Gly6 motif.[15] This transition requires an activated torsional motion, that is, a $+120^{\circ}$ rotation around the Gly6 ϕ torsional angle, which is characterized by a rate constant of $3.1\times10^{6}\ s^{-1}$ (320 ns).[7] This approach was applied here for investigating the conformational and dynamic properties of the ion–peptide complexes formed by Ca^{II} and Gd^{III} with the aforementioned TrGA fluorescent analogues.

Results and Discussion

CD measurements

CD spectra in acetonitrile of both TrGA analogues F0 and F0T8 show a negative band at 204–205 nm and a weaker negative band at 220–230 nm (Figures 1 and 2); this profile is typical of oligopeptides populating preferentially helical conformations.[20,21] Binding of Ca^{II} and Gd^{III} gives rise to a conformational transition for both of the peptide analogues, as clearly revealed by the CD spectra of F0–Ca^{II}, F0–Gd^{III}, F0T8–Ca^{II} and F0T8–Gd^{III} at the different metal ion–peptide total molar concentration ratios ($r=[Me]_t/[P]_t$) reported in Figures 1 and 2. At high r values, the CD curves of all ion–peptide complexes investigated show a positive maximum at 214–218 nm, which is typical of structures rich in type II β turns.[22–24] Gurunath and Balaram[25] analyzed the conformational features of the C-terminal heptapeptide segment of TrGA by CD spectroscopy and NMR Overhauser effect experiments, and concluded that the positive CD signal at 212 nm could be assigned to nonhelical, folded structures generated by multiple β turns, as proved in particular by the occurrence of a series of NMR contacts. Most probably, ion binding selects the appropriate values out of the many possible torsional angles and stabilizes β-turn structures. The quasi-isodichroic point found for all systems between 196 and 202 nm indicates that the CD spectra essentially result from the overlap of two spectral contributions. This conclusion is strengthened by the observation that the CD signal at all wavelengths can be accounted for by weighting appropriately the CD curves typical of the free peptide ($r=0$) and of the ion–peptide complex at high r. It is worth noting that, while the peptide complexes with Ca^{II} show molar ellipticities at 214–216 nm around $3\times10^{4}\ deg\,cm^{2}\,dmol^{-1}$, the Gd^{III}–peptide complexes exhibit definitely higher CD values ([Θ]

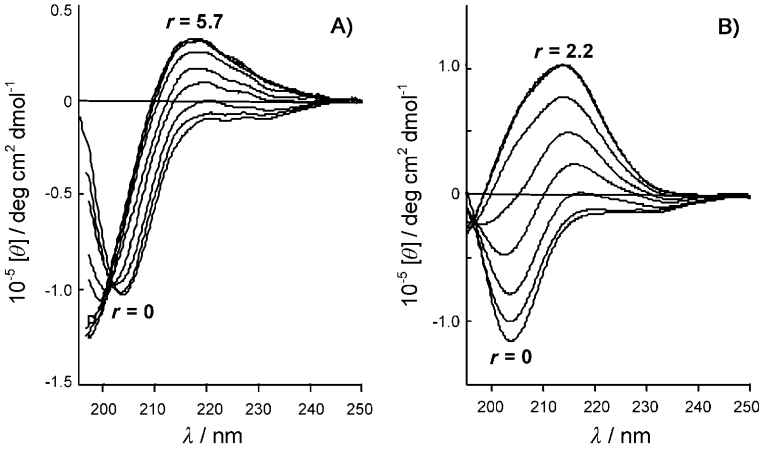

Figure 1. CD spectra of F0 in acetonitrile with increasing concentrations of A) Ca^{II} and B) Gd^{III}; $[F0]=10^{-4}$ M, $[Ca^{II}]=0–5.7\times10^{-4}$ M, $[Gd^{III}]=0–2.2\times10^{-4}$ M, r = [metal ion]/[peptide] total molar concentration ratio.

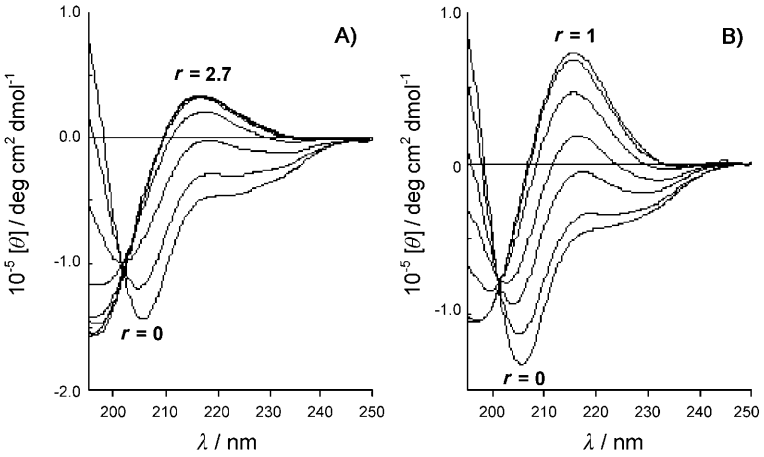

Figure 2. CD spectra of F0T8 in acetonitrile with increasing concentrations of A) Ca^{II} and B) Gd^{III}; $[F0T8]=10^{-4}$ M, $[Ca^{II}]=0–2.7\times10^{-4}$ M, $[Gd^{III}]=0–1\times10^{-4}$ M, r = [metal ion]/[peptide] total molar concentration ratio.

$\approx 10^5$ deg cm^2 dmol^{-1}); this suggests a larger conformational effect of the threefold charged Gd^{III}.[26] Interestingly, titration experiments with alkaline ions (Na^+, K^+) did not reveal perturbations in the CD spectra of either the F0 or F0T8 analogue (see the Supporting Information), thus revealing the specific character of the ion–peptide interaction. The normalized CD molar ellipticities at 218 nm versus r ($=[Me]_t/[P]_t$) are reported in Figure 3 for the complexes that F0T8 formed with Ca^{II} and

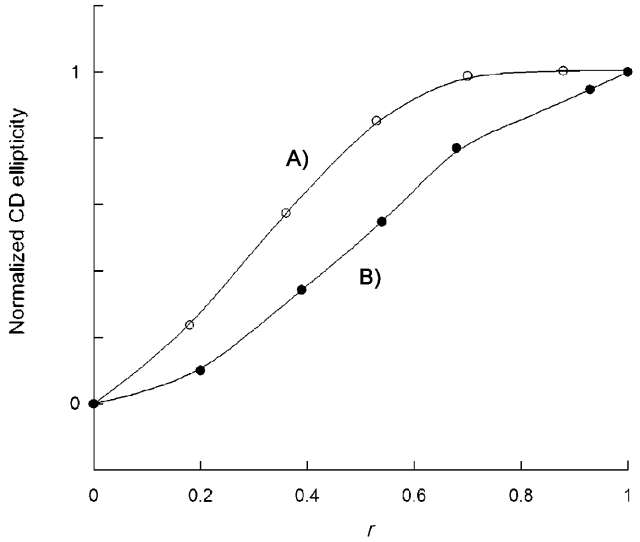

Figure 3. Relative variation of the CD molar ellipticity at $\lambda = 218$ nm in response to various metal ion–peptide concentration ratios, r; A) F0T8–Ca^{II}; B) F0T8–Gd^{III}.

Gd^{III}. These data show that the peptide conformational transition is almost completed at $r = 1$; this indicates the formation of a 1:1 metal ion–peptide complex at saturating conditions. From the same Figure, some differences in the binding of the two ions to F0T8 can be noticed, in contrast to what was observed for F0 (data not shown). This finding could indicate a structural role for the TOAC group of F0T8 in the proximity of the ion binding site.

Fluorescence experiments

We have recently investigated the distance dependence of the excited state interaction between the fluorescent Fmoc group and the TOAC nitroxide quencher for a series of TrGA analogues.[14,15] It has been shown that for Fmoc···TOAC centre-to-centre distances longer than 4–5 Å, the Förster dipole–dipole interaction model[27] adequately describes the excited state interaction between the aromatic molecule and the nitroxyl radical quencher.[28] At shorter distances, the overlap of the electronic distributions gives rise to ultrafast relaxation mechanisms that completely deplete the fluorescence emission. Time-resolved fluorescence experiments have been performed to study the peptide conformational and dynamic properties in the nanosecond time region. The singlet excited-state time decays is usually described by a sum of exponential time components [Eq. (1)]:

$$I(t) = \sum_{i=1}^{n} \alpha_i \exp(-\tfrac{t}{\tau_i}) \quad (1)$$

where α_i is the weight associated to the ith lifetime, τ_i. Provided that the different conformers do not interconvert in the nanosecond time scale so that dynamic averaging of the instantaneous relative positions of the donor and acceptor pair cannot take place, each decay time component can be associated to a specific conformer.[15] Furthermore, in the absence of ground-state interactions, the experimental pre-exponential factor, α_i, can be directly associated to the Boltzmann-weighted population of each conformer.[29] An alternative procedure describes the experimental time decays by continuous lifetime distributions, each representing a family of structurally similar conformations.[30]

Besides structural factors, the width of the distribution depends on the interconversion dynamics among the different conformers pertaining to the same family.

Fluorescence steady-state quantum yields and time decay parameters (τ_1 and τ_2) for F0 and F0T8 and their complexes with Ca^{II} and Gd^{III} in acetonitrile at saturating ion–peptide concentration ratios are reported in Table 1. It can be seen that for

Table 1. Fluorescence parameters for the two trichogin GA IV analogues and their complexes with Ca^{II} and Gd^{III} in acetonitrile.

Peptide	Quantum yield	α_1	τ_1 [ns]	α_2	τ_2 [ns]	E_1	E_2
F0	0.42	–	5.9	–	–		
F0–Ca^{II}	0.46	–	5.9	–	–		
F0–Gd^{III}	0.44	–	5.9	–	–		
F0T8	0.26	0.14	2.4	0.86	4.7	0.59	0.20
F0T8–Ca^{II}	0.27	0.27	2.1	0.73	5.4	0.64	0.08
F0T8–Gd^{III}	0.26	0.47	1.85	0.53	5.5	0.69	0.07

F0 the binding of both metal ions does not affect the Fmoc emission. The absence of excited state interactions between the Fmoc fluorene chromophore and Ca^{II} or Gd^{III} was confirmed by independent fluorescence quenching experiments performed with a Fmoc derivative and the two metal ions freely diffusing in solution. Hence, we can safely conclude that the effect of the ion binding on the time decay observed for F0T8 is not ascribable to a photophysical interaction between the fluorene group and the metal ion, but it reflects the changes in the relative distances and orientations of the Fmoc···TOAC donor (D)–acceptor (A) pair in the free F0T8 and in the F0T8 complexes with Gd^{III} or Ca^{II}; this finding corroborates the structural changes of the peptide backbone revealed by CD experiments. From the data reported in Table 1, it can be seen that the fluorescence time decays of F0T8 and its complexes with Ca^{II} and Gd^{III} can be described by two lifetime components. A lifetime distribution analysis (those for F0T8 and F0T8–Gd^{III} are reported in Figure 4) confirms that—in close similarity with F0T8—the ion–peptide complexes populate two distinct families of conformers. This finding, together with the CD results, supports the view of the onset of a conformational

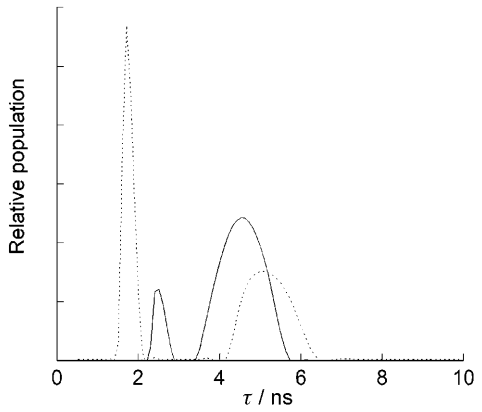

Figure 4. Lifetime distributions from time-resolved fluorescence experiments in acetonitrile; ——: F0T8; -----: F0T8–Gd.

equilibrium between two conformers (or two families of very similar conformers interconverting on the nanosecond time scale) characterized by a longer and a shorter lifetime (or lifetime distributions), as a result of the different relative distances and orientations of the Fmoc···TOAC D···A pair. This situation is reminiscent of that we already found for F0T8 in methanol solution.[14,15] From the data reported in Table 1 and from inspection of Figure 4, we can also argue that this conformational equilibrium is strongly affected by the ion binding process. In particular, the pre-exponential factor α_1 increases from 0.14 for the free peptide ($\alpha_2 = 0.86$) to 0.27 for the F0T8–Ca^{II} complex ($\alpha_2 = 0.73$) and 0.47 for F0T8–Gd^{III} ($\alpha_2 = 0.53$). Furthermore, the ion binding moves the long and short time components of the F0T8 fluorescence decay to longer and shorter lifetimes, respectively, as a result of the structural changes of the peptide scaffold upon ion coordination. The last two columns of Table 1 report the experimental quenching efficiencies (E_1 and E_2) associated with the two time decays (it is worth noting that the maxima of the lifetime distributions shown in Figure 4 coincide, within the experimental resolution, with the discrete lifetimes reported in Table 1) according to Equation (2):

$$E_m^{exp} = 1 - \frac{\tau_m}{\tau_0} \qquad (2)$$

where τ_0 is the lifetime of the reference compound F0. These experimental quantities can be directly compared with the theoretical efficiencies computed from the molecular structures obtained by the MM calculations described below.

Conformational analysis by molecular mechanics calculations

MM calculations were carried out to obtain structural information on the conformations predominantly populated in solution by the ion–peptide complexes. In a series of papers we have shown that time-resolved FRET experiments and theoretical conformational analysis can be jointly applied to determine the conformational properties of sterically constrained oligopeptides in solution.[28] According to the Förster model,[27] the energy transfer quenching efficiency is given by Equation (3), where R_m and k_m^2 are the D···A centre-to-centre distance and the D···A orientation factor in the *m*th conformer, respectively.

$$E_m^{th} = \frac{1}{1+\frac{2}{3k_m^2}\left(\frac{R_m}{R_0}\right)^6} \qquad (3)$$

R_0 is a pure spectroscopic quantity characteristic of the D···A pair and represents the distance at which 50% transfer of excitation energy takes place for a randomly oriented energy transfer pair ($k_m^2 = {}^2/_3$).[15,29] For the Fmoc···TOAC pair in acetonitrile, R_0 is equal to 10.7 Å, as determined by spectroscopic measurements. Therefore, the comparison of experimental [Eq. (1)] and theoretical [Eq. (3)] quenching efficiencies allow us to validate the conformational structures provided by MM calculations. A detailed MM analysis of the conformational features of F0T8 in methanol, which were performed previously, showed that this peptide maintains the mixed $3_{10}/\alpha$-helix structure observed by X-ray diffraction and NMR spectroscopy experiments on TrGA (denoted in the following as conformer A).[15] Compact 3D structures, in which the two N-terminal (1 to 4) and C-terminal (7 to 11) helical segments are brought to close proximity by the turn formed around the Aib4-Gly5-Gly6 residues, were also found to be significantly populated (conformer B).[15] These conformers were associated with the longer and shorter lifetime components of the F0T8 fluorescence time decay, respectively. MM calculations on the metal ion–peptide complexes show that ion binding causes a partial disruption of the helical segment at the C terminus of conformer A. The terminal residues strongly coordinate the metal ion, and form a loop that encloses the positive charge through interactions with the peptide C=O groups positioned in a pseudo-octahedral arrangement (Figure 5 for the F0T8–Ca^{II} complex; Figure 6 for the F0T8–Gd^{III} complex). The role of the Gly5-Gly6 residues is particularly relevant for conformer B and gives rise to a twist of the backbone that brings the C- and N-terminal helices to collapse in a compact structure that embeds the ion ligand (Figure 5, lower panel for the F0T8–Ca^{II} complex; Figure 6, lower panel for the F0T8–Gd^{III} complex); this arrangement mimics the helix-turn-helix motif usually found in calcium-binding proteins and peptides.[16,17]

In Table 2 we report the centre-to-centre distance (d_m) and relative orientation (k_m^2) of the Fmoc···TOAC pair, along with the theoretical efficiency (E_m^{th}) and the Boltzmann-weighted population (P_m) for the low-energy conformers of the bare peptide and the peptide complexes with Ca^{II} and Gd^{III}. While the calculated quenching efficiencies are in very good agreement with the associated experimental quantities, the relative populations of the two conformers are somewhat more scattered with respect to the experimental data, due to the sensitivity of the Boltzmann factor weighting the conformational energies. In the computed structures of the ion–peptide complexes the Gd^{III} ion appears to be deeply embedded in the peptide scaffold and coordinates more tightly to a larger number of carbonyl groups, as clearly shown in the structures reported in Figure 6 for both conformers A and B. This finding, which most likely reflects the larger electrostatic contribution of the threefold charged Gd^{III} with respect to Ca^{II}, could explain

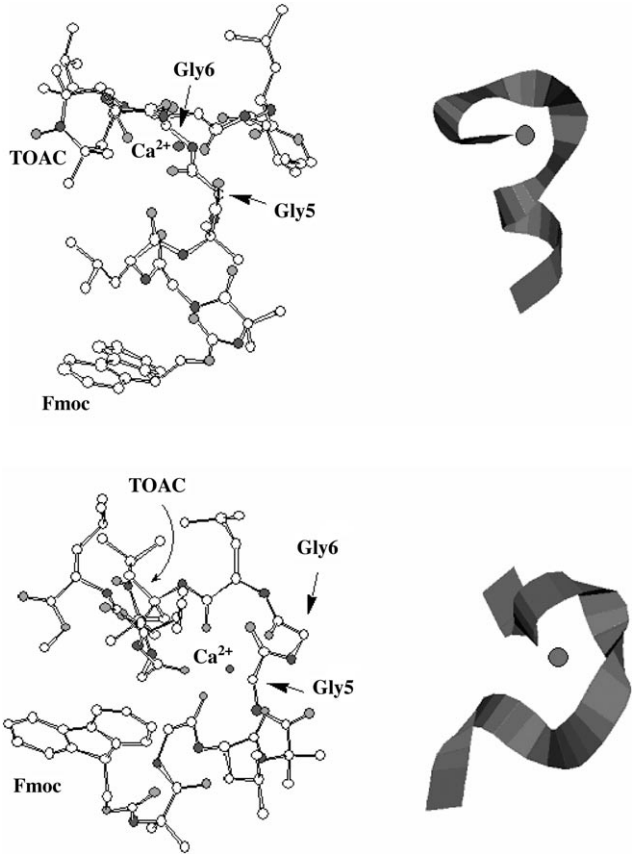

Figure 5. The most stable conformers of F0T8–Ca^{II} from MM calculations (top panel: conformer A; lower panel: conformer B). White spheres: carbon atoms; dark grey: nitrogen; light grey: oxygen. The position of the metal ion is also indicated. Hydrogen atoms are omitted for clarity. To the right a ribbon representation of the backbone structure is also shown.

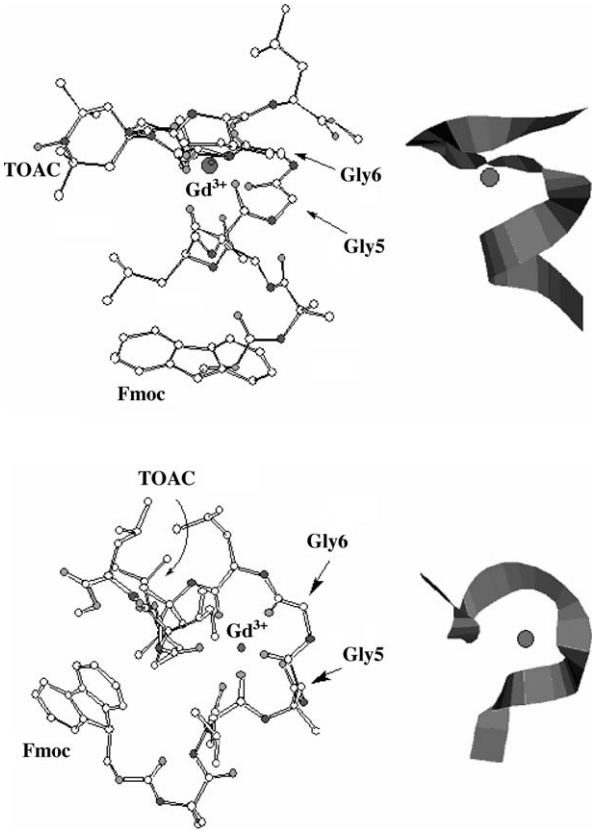

Figure 6. The most stable conformers of F0T8–Gd^{III} from MM calculations (top panel: conformer A; lower panel: conformer B). White spheres: carbon atoms; dark grey: nitrogen; light grey: oxygen. The position of the metal ion is also indicated. Hydrogen atoms are omitted for clarity. To the right a ribbon representation of the backbone structure is also shown.

the differences between the complexes that F0 and F0T8 form with the two ion ligands, as revealed by CD experiments and, for the latter peptide, by time-resolved fluorescence experiments as well. It should be noted here that, despite the structural differences revealed by the CD and fluorescence time-resolved experiments, the topology of the two conformations differently populated by the bare peptides and the ion–peptide complexes is essentially the same, as indicated by the quasi-isosbestic point in the CD experiments, the similar time distributions in the time resolved fluorescence experiments and the conformational features obtained by MM calculations.

Table 2. Centre-to-centre distance (d_m), relative orientation (k^2_m), theoretical quenching efficiency (E^{th}_m), and population (P_m) of the low-energy conformers A and B for the two trichogin GA IV analogues and their complexes with Ca^{II} and Gd^{III} from MM calculations.

Peptide	d_m [Å]	k^2_m	E^{th}_m	P_m
F0T8 (A)	14.5	0.79	0.16	0.58
F0T8 (B)	10.0	0.53	0.54	0.38
F0T8–Ca^{II} (A)	11.6	0.02	0.02	0.85
F0T8–Ca^{II} (B)	9.7	0.79	0.68	0.12
F0T8–Gd^{III} (A)	12.6	0.04	0.02	0.60
F0T8–Gd^{III} (B)	8.1	0.32	0.72	0.37

Transient absorption experiments and peptide dynamics

The quenching process of the Fmoc triplet state by TOAC allowed us to obtain information on the peptide dynamics in the microsecond time scale. This is because the triplet state quenching mechanism requires that the Fmoc···TOAC pair approaches contact distances and is therefore governed by diffusional motions of the peptide chain.[31] The Fmoc···TOAC bimolecular quenching constant, as determined by intermolecular quenching experiments in solution, is $1.3\times10^9\,M^{-1}s^{-1}$, that is, close to the diffusion limit. Therefore, once the two probes attain a short separation distance, quenching of the Fmoc triplet state occurs almost instantaneously; this allows one to determine the rate for achieving contact distances between the two probes in F0T8.[14] Binding of Ca^{II} or Gd^{III} to F0T8 dramatically affects the peptide dynamics, as it is clearly shown by the time decays reported in Figure 7. The associated kinetic parameters, as obtained by a bi-exponential fit of the kinetic trace at a fixed wavelength (Table 3), reveal that in the F0T8 complexes with Ca^{II} and Gd^{III} the observed decay constants are strongly depleted and become almost equal to the values obtained for the complexes that Gd^{III} and Ca^{II} form with the reference peptide F0, which lacks the TOAC quencher. The faster decay component was unambiguously assigned to the Fmoc triplet state

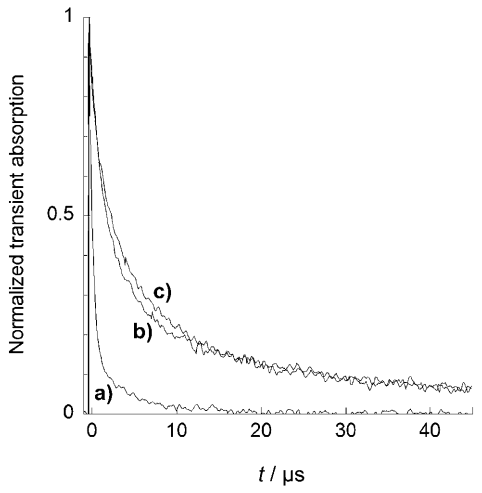

Figure 7. Transient absorption decays of A) F0T8; B) F0T8–[Ca^{II}]; C) F0T8–[Gd^{III}] in acetonitrile; $\lambda = 370$ nm, $T = 25\,^{\circ}C$.

Table 3. Fmoc transient absorption decay parameters in acetonitrile for the two trichogin GA IV analogues and their complexes with Ca^{II} and Gd^{III}.

Peptide	α_1	k_1 [$10^5\ s^{-1}$]	α_2	k_2 [$10^4\ s^{-1}$]
F0	0.28	1.9	0.72	4.1
F0–Ca^{II}	0.15	1.9	0.85	3.0
F0–Gd^{III}	0.09	2.6	0.91	3.1
F0T8	0.72	22.8	0.28	19.2
F0T8–Ca^{II}	0.62	4.7	0.38	5.9
F0T8–Gd^{III}	0.45	5.3	0.55	9.6

decay by oxygen quenching experiment.[6] Assuming $k_{obs} = k_0 + k_d$, where k_0 is the triplet decay rate constant in the absence of the quencher and k_d is the unimolecular rate characterizing the diffusional motions that bring the Fmoc···TOAC pair to very close proximity, it turns out that the F0T8 dynamics ($k_d^{-1} =$ 480 ns) is markedly slowed down for both the F0T8 complexes with Ca^{II} ($k_d^{-1} = 3.6$ μs) and Gd^{III} ($k_d^{-1} = 3.7$ μs). Most likely, the binding of Ca^{II} and Gd^{III} slows down the torsional motions of the peptide backbone and brings the Fmoc···TOAC pair into close proximity; this rigidity, however, inhibits the quenching of the Fmoc triplet state. The ion–peptide structures reported in Figures 5 and 6 clearly support this finding and emphasize the role of the hinge residues Gly5-Gly6 in the formation of the peptide loop that embeds the ion ligands.

Water–membrane partition experiments

Binding experiments, which were based on the enhancement of Fmoc emission when inserted in an apolar environment, were performed by adding a liposome formulation to F0 and the complex F0–Gd^{III}. The water–membrane partition properties of the peptide are not affected by coordination of the metal ion, the association constant to the liposomes being $K = (1.6 \pm 0.1) \times 10^3$ for F0 and $(1.7 \pm 0.1) \times 10^3$ for the complex F0–Gd^{III}.

To verify that Gd^{III} effectively penetrates the liposome, a spectrophotometric assay based on Arsenazo III was carried out.[32] This dye exhibits a very high affinity to Gd^{III} and an extremely sensitive variation of its absorption spectrum to ion binding. In brief, the experiment consists of preparing two liposome solutions dipped in the upper section of two different centrifugal filter devices. Upper and lower sections are separated by a cellulose membrane that is only permeable to molecules with molecular weights lower than 100 kDa. The complex F0–Gd^{III} is added to one of the filter devices, while in the other only Gd^{III} at the same concentration is inserted. Then, ultracentrifugation is applied to both solutions to separate the aqueous layer from the lipids. Finally, the concentration of Gd^{III} passed to the lower section of both filters is measured by complexation with Arsenazo III. A definitely lower concentration of Gd^{III} was found in the case of F0–Gd^{III} (1.56 mM) with respect to that measured in the reference cell (2.67 mM). This result indicates that an important fraction of the complex F0–Gd^{III} was segregated in the upper section, bound to the liposome phase.

Conclusions

Two fluorescent peptide analogues of TrGA were synthesized and their binding properties with Ca^{II} and Gd^{III} ions were characterized by CD, time resolved optical spectroscopy, and MM calculations. The last methodology revealed that both of the conformers predominantly populated by the bare peptide are able to bind the two metal ions. Ion binding promotes a shift in the conformational equilibrium and gives rise to a peptide loop that embeds the metal ion into a binding cavity formed by carbonyl groups. Peptide dynamics is also strongly affected by ion binding: the peptide torsional motions were slowed down to the microsecond time scale. The effective coordination with Ca^{II} and Gd^{III} of the TrGA analogues investigated, and their high affinity to the lipid phase strongly suggest that these peptides could be used as Trojan horses to insert Gd^{III}, which is a well-known magnetic probe, into the membrane. These properties are particularly important for the high contrast capacity of Gd^{III} ions in NMR imaging when embedded in a lipid phase.[33] Preliminary, unpublished results (Arsenazo III assay) have confirmed the feasibility of this approach. In addition, by taking advantage from the presence of the Fmoc group, these peptides could also be of real interest in biological and medical assays by using optical (fluorescence) imaging.

Experimental Section

The synthesis and chemical characterization of the TrGA analogues F0 and F0T8 were already reported.[34] CD spectroscopy experiments were carried out by using a Jasco J-600 (Tokyo, Japan) dichrograph. The reported CD signals were normalized with respect to peptide molar concentrations. Fluorescence spectra were recorded by using a Jobin Yvon Fluoromax-2 (Longjumeau, France) spectrofluorimeter operating with single photon counting (SPC) detection. Fluorescence time decays were measured by a CD900 SPC apparatus from Edinburgh Analytical Instruments (Edinburgh, Scotland, UK). UV excitation was achieved by a flashlamp filled

with ultrapure hydrogen (300 mm Hg; 40 kHz repetition rate; full width at half maximum: 1.1 ns). The experimental decays were fitted through iterative reconvolution of discrete exponential functions or continuous lifetime distributions by using standard software licensed by Edinburgh Analytical Instruments. Transient absorption experiments were performed with an Applied Photophysics LKS60 instrument (Leatherhead, UK), by using a Quantel Brilliant B Nd:YAG Q-switched laser (Les Uils, France) for pump excitation. A fourth-harmonic generator module was employed to obtain a 266 nm excitation wavelength (4 ns pulse width; 10 mJ energy). All solutions for spectroscopy experiments were freshly prepared before measurement. Spectrograde solvents (Carlo Erba, Rodano, Italy) were exclusively used. To determine the Gd^{III} concentration associated to liposomes, a spectrophotometric assay, based on Arsenazo III, was carried out by measuring the absorption of the ion–dye complex at 660 nm. Centrifugation was performed with an ALC PK110 centrifuge at 6000 rpm for 50 min by using Microcon Eppendorfs with a regenerated cellulose filter. Phospholipids were purchased from Avanti Polar Lipids (Alabaster, AL, USA). The procedure for liposome preparation has already been reported.[35] MM calculations were carried out by using a homemade program linked to Hyperchem 7.0,[36] with a MM+ force field implemented with the TOAC parameters.[37]

Acknowledgements

This project was supported by the Italian Ministry of University and Research (PRIN 2006) and in part by the Italian Ministry of Foreign Affairs.

Keywords: circular dichroism · ion–peptide complexes · lipopeptaibol antibiotics · peptides · time-resolved fluorescence

[1] S. Rebuffat, C. Goulard, B. Bodo, M. T. Roquebert, *Recent Res. Devel. Org. Bioorg. Chem.* **1999**, *3*, 65–91.
[2] C. Toniolo, M. Crisma, F. Formaggio, C. Peggion, R. F. Epand, R. M. Epand, *Cell. Mol. Life Sci.* **2001**, *58*, 1179–1188.
[3] C. Peggion, F. Formaggio, M. Crisma, R. F. Epand, R. M. Epand, C. Toniolo, *J. Pept. Sci.* **2003**, *9*, 679–689.
[4] C. Toniolo, *Biopolymers* **1989**, *28*, 247–257.
[5] C. Toniolo, M. Crisma, G. M. Bonora, E. Benedetti, B. Di Blasio, V. Pavone, C. Pedone, A. Santini, *Biopolymers* **1991**, *31*, 129–138.
[6] I. L. Karle, P. Balaram, *Biochemistry* **1990**, *29*, 6747–6756.
[7] C. Toniolo, M. Crisma, F. Formaggio, C. Peggion, *Biopolymers* **2001**, *60*, 396–419.
[8] C. Toniolo, E. Benedetti, *Trends Biochem. Sci.* **1991**, *16*, 350–353.
[9] C. M. Venkatachalam, *Biopolymers* **1968**, *6*, 1425–1436.
[10] C. Toniolo, C. Peggion, M. Crisma, F. Formaggio, X. Shui, D. S. Eggleston, *Nat. Struct. Biol.* **1994**, *1*, 908–914.
[11] C. Auvin-Guette, S. Rebuffat, Y. Prigent, B. Bodo, *J. Am. Chem. Soc.* **1992**, *114*, 2170–2174.
[12] C. Toniolo, M. Crisma, F. Formaggio, C. Peggion, V. Monaco, C. Goulard, S. Rebuffat, B. Bodo, *J. Am. Chem. Soc.* **1996**, *118*, 4952–4958.
[13] V. Monaco, E. Locardi, F. Formaggio, M. Crisma, S. Mammi, E. Peggion, C. Toniolo, S. Rebuffat, B. Bodo, *J. Pept. Res.* **1998**, *52*, 261–272.
[14] M. Venanzi, E. Gatto, G. Bocchinfuso, A. Palleschi, L. Stella, F. Formaggio, C. Toniolo, *ChemBioChem* **2006**, *7*, 43–45.
[15] M. Venanzi, E. Gatto, G. Bocchinfuso, A. Palleschi, L. Stella, C. Baldini, F. Formaggio, C. Toniolo, *J. Phys. Chem. B* **2006**, *110*, 22834–22841.
[16] H. S. Atreya, S. C. Sahu, A. Bhattacharya, K. V. R. Chary, G. Govil, *Biochemistry* **2001**, *40*, 14392–14403.
[17] B. Kuhlman, J. A. Boice, W.-J. Wu, R. Fairman, D. P. Raleigh, *Biochemistry* **1997**, *36*, 4607–4615.
[18] S. M. Mustafi, S. M. Mukherjee, K. V. R. Chary, C. Del Bianco, C. Luchinat, *Biochemistry* **2004**, *43*, 9320–9331.
[19] C. Gløgård, G. Stensrud, R. Hovland, S. L. Fossheim, J. Klaveness, *Int. J. Pharm.* **2002**, *233*, 131–140.
[20] C. Toniolo, A. Polese, F. Formaggio, M. Crisma, J. Kamphuis, *J. Am. Chem. Soc.* **1996**, *118*, 2744–2745.
[21] F. Formaggio, M. Crisma, P. Rossi, P. Scrimin, B. Kaptein, Q. B. Broxterman, J. Kamphuis, C. Toniolo, *Chem. Eur. J.* **2000**, *6*, 4498–4504.
[22] R. W. Woody, *The Peptides, Vol. 7* (Ed.: V. J. Hruby), Academic, New York, **1985**, pp. 15–114.
[23] G. D. Rose, L. M. Gierasch, J. A. Smith, *Adv. Protein Chem.* **1985**, *37*, 1–109.
[24] A. Perczel, M. Hollosi, B. M. Foxman, G. D. Fasman, *J. Am. Chem. Soc.* **1991**, *113*, 9772–9784.
[25] R. Gurunath, P. Balaram, *Biopolymers* **1995**, *35*, 21–29.
[26] J. Wójcik, J. Góral, K. Pawłoski, A. Bierzyński, *Biochemistry* **1997**, *36*, 680–687.
[27] T. Förster, *Discuss. Faraday Soc.* **1959**, *27*, 7–17.
[28] B. Pispisa, C. Mazzuca, A. Palleschi, L. Stella, M. Venanzi, M. Wakselman, J.-P. Mazaylerat, M. Rainaldi, F. Formaggio, C. Toniolo, *Chem. Eur. J.* **2003**, *9*, 4084–4093, and references therein.
[29] B. Pispisa, A. Palleschi, M. Venanzi, G. Zanotti, *J. Phys. Chem.* **1996**, *100*, 6835–6844.
[30] J. R. Lakowicz, *Principles of Fluorescence Spectroscopy*, Springer, New York, **2006**, Chapter 4.
[31] L. J. Lapidus, W. A. Eaton, J. Hofrichter, *Proc. Natl. Acad. Sci. USA* **2000**, *97*, 7220–7225.
[32] G. Weissmann, P. Anderson, C. Serhan, E. Samuelsson, E. Goodman, *Proc. Natl. Acad. Sci. USA* **1980**, *77*, 1506–1510.
[33] P. Caravan, J. J. Ellison, T. J. McMurry, R. B. Lauffer, *Chem. Rev.* **1999**, *99*, 2293–2352.
[34] V. Monaco, F. Formaggio, M. Crisma, C. Toniolo, P. Hanson, G. L. Millhauser, *Biopolymers* **1999**, *50*, 239–253.
[35] E. Gatto, C. Mazzuca, L. Stella, M. Venanzi, B. Pispisa, *J. Phys. Chem. B* **2006**, *110*, 22813–22818.
[36] Hyperchem Computational Chemistry, Hypercube Inc., Gainesville, FL, **2002**.
[37] V. Barone, A. Bencini, M. Cossi, A. Di Matteo, M. Matterini, F. Totti, *J. Am. Chem. Soc.* **1998**, *120*, 7069–7078.

Received: September 11, 2008
Published online on December 9, 2008

